

Supplementary Materials

Cotransport of Cu with Graphene Oxide in Saturated Porous Media with Varying Degrees of Geochemical Heterogeneity

Jianzhou He¹, Dengjun Wang^{2,*}, Tingting Fan^{1,3}, Dongmei Zhou^{1,4,*}

¹ Key Laboratory of Soil Environment and Pollution Remediation, Institute of Soil Science, Chinese Academy of Sciences, Nanjing 210008, China

² Oak Ridge Institute for Science and Education (ORISE) Resident Research Associate at the U.S. Environmental Protection Agency, Ada, Oklahoma 74820, United States

³ Nanjing Institute of Environmental Science, Ministry of Ecology and Environment of the People's Republic of China, Nanjing 210042, China

⁴ State Key Laboratory of Pollution Control & Resource Reuse, School of Environment, Nanjing University, Nanjing 210023, China

*Corresponding Authors:

Dengjun Wang; Tel.: +1 (580) 436-8828; Fax: +1 (580) 436-8703;

Email: wang.dengjun@epa.gov.

Dongmei Zhou; Tel.: +86-25-86881180; Fax: +86-25-86881000;

Email: dmzhou@issas.ac.cn.

Text S1. The zeta potentials of heterogeneous mixtures

The zeta potentials of heterogeneous mixtures (uncoated and Fe oxide coated sand grains) were calculated using an empirical equation reported in literature [1,2], as follows:

$$\zeta_C = \omega\zeta_{Fe\ oxides} + (1 - \omega)\zeta_{sand}$$

where ζ_C is the overall zeta potential of the collectors, ω is the portion of Fe oxide coated sand, $\zeta_{Fe\ oxides}$ and ζ_{sand} are the zeta potentials of the Fe oxides and the sand colloids, respectively, which were measured using a NanoBrook 90Plus PALS analyzer (Brookhaven, US).

Text S2. Analysis for Cu

Before experiments, we compared two different methods for a good separation of dissolved Cu^{2+} from bulk solution in the presence of GO. The mixture of GO and $CuCl_2$ was centrifuged at $11,000 \times g$ for 30 min, and then filtered through a 0.22- μm membrane filter. Comparably, a Amicon Ultra-30kD membrane filter (Millipore, US) was applied to separate dissolved Cu in the aqueous suspension. The filter device was spun at $45,000 \times g$ for 20 min. The concentrations of Cu in filtrates were analyzed using an atomic absorption spectrophotometer (AAS, Hitachi Z-2000, Japan). The results showed no significant difference with regard to the detected Cu in Figure S2.

Text S3. Langmuir fitting for the adsorption isotherm

In order to describe the adsorption behavior of Cu^{2+} on GO, the isotherm was fitted using Langmuir model as follow:

$$Q_e = \frac{Q_{max}k_L C_e}{1 + k_L C_e}$$

where Q_e is the amount of Cu adsorbed on GO at equilibrium ($mg\ g^{-1}$), Q_{max} is the maximum adsorption capacity ($mg\ g^{-1}$), k_L is the Langmuir sorption coefficient ($L\ mg^{-1}$), C_e is the equilibrium concentration of Cu^{2+} in aqueous solution ($mg\ L^{-1}$).

Text S4. Numerical Model

A one-dimensional form of the convection-dispersion equation with two types of kinetic retention sites [3,4] has been successfully applied to simulate the transport of GO in saturated sand covered with iron oxides, biofilms, and extracellular polymeric substances [5,6], as below:

$$\frac{\partial \theta C}{\partial t} + \rho_b \frac{\partial (S_1)}{\partial t} + \rho_b \frac{\partial (S_2)}{\partial t} = \frac{\partial}{\partial x} \left(\theta D \frac{\partial C}{\partial x} \right) - \frac{\partial q C}{\partial x} \quad (\text{S1})$$

where θ is the volumetric water content [-], C is the GO concentration in the aqueous phase [N L^{-3} , where N and L denote number and length, respectively], t is the time [T], ρ_b is the bulk density of the porous matrix [M L^{-3} , where M denotes the unit of mass], x is the vertical spatial coordinate [L], D is the hydrodynamic dispersion coefficient [$\text{L}^2 \text{T}^{-1}$], q is the Darcy velocity [L T^{-1}], and S_1 [N M^{-1}] and S_2 [N M^{-1}] are the solid-phase concentration associated with retention sites 1 and 2, respectively.

The two kinetic retention sites described mass transfer of GO between aqueous and solid phases. The first kinetic site (site 1, Eq. S2) assumes reversible retention, whereas the second kinetic site (site 2, Eq. S3) assumes irreversible and time-dependent retention as:

$$\rho_b \frac{\partial (S_1)}{\partial t} = \theta k_1 C - \rho_b k_{1d} S_1 \quad (\text{S2})$$

$$\rho_b \frac{\partial (S_2)}{\partial t} = \theta k_2 \psi_t C \quad (\text{S3})$$

where k_1 [T^{-1}] and k_2 [T^{-1}] are first-order retention coefficients on sites 1 and 2, respectively, k_{1d} [T^{-1}] is the first-order detachment coefficient, and ψ_t is a dimensionless function to account for time-dependent retention [-]. The value of ψ_t is given as [7]:

$$\psi_t = 1 - \frac{S_2}{S_{\max 2}} \quad (\text{S4})$$

where $S_{\max 2}$ [N M^{-1}] is the maximum solid-phase concentration of GO on site 2.

Figure S1.

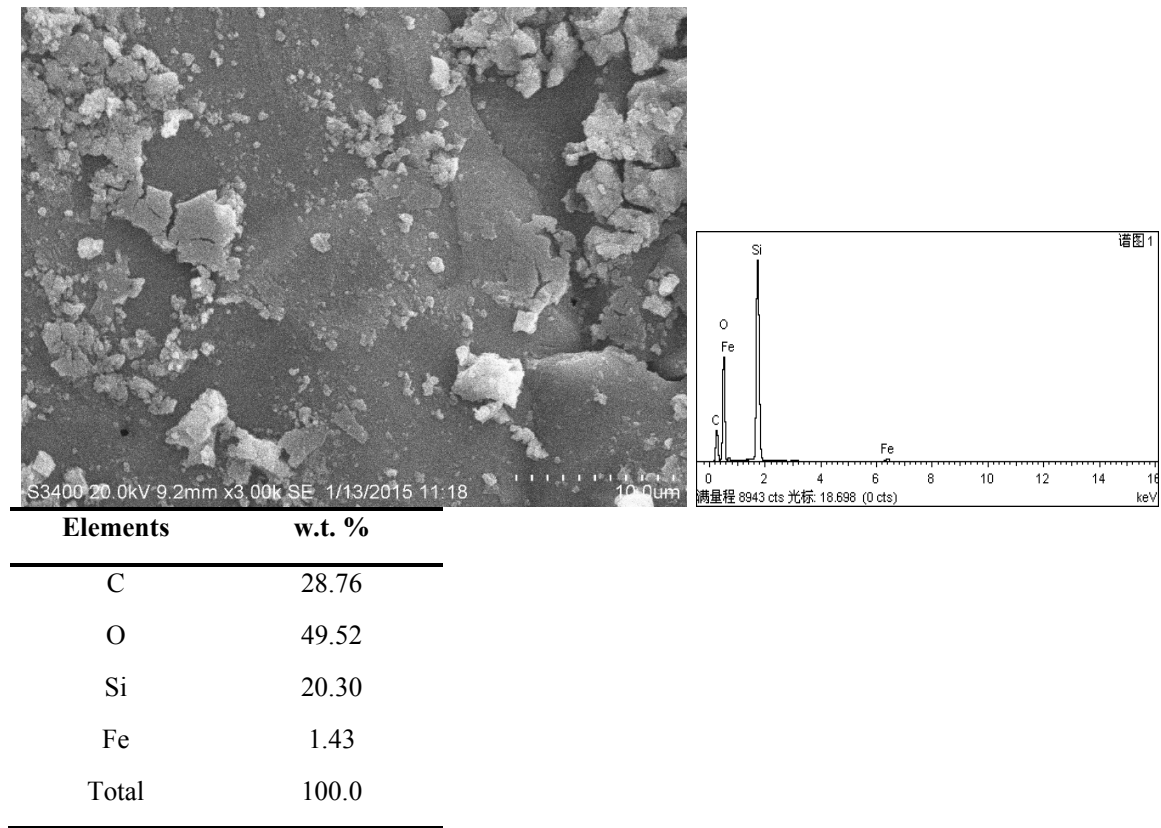


Figure S1. Selected SEM image of Fe oxide coated quartz sand used in the study and the corresponding energy dispersive x-ray spectroscopy for elemental composition analysis.

Figure S2.

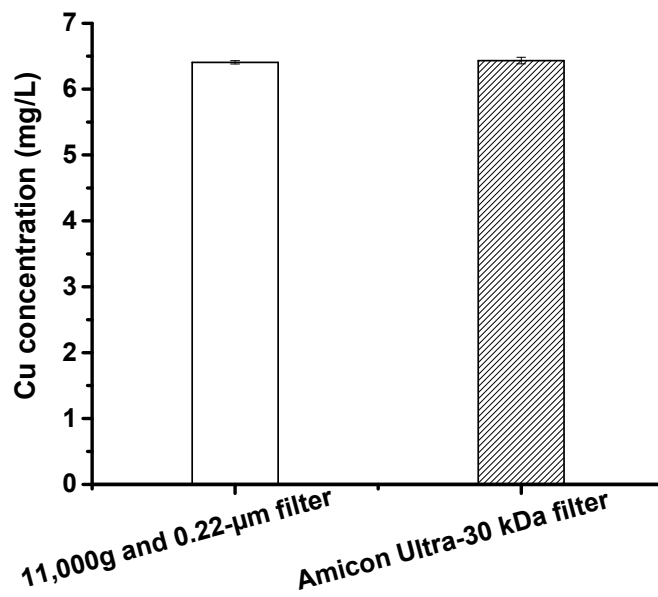


Figure S2. Method comparison for separating dissolved Cu^{2+} from bulk solution in the presence of 20 mg L^{-1} GO.

Figure S3.

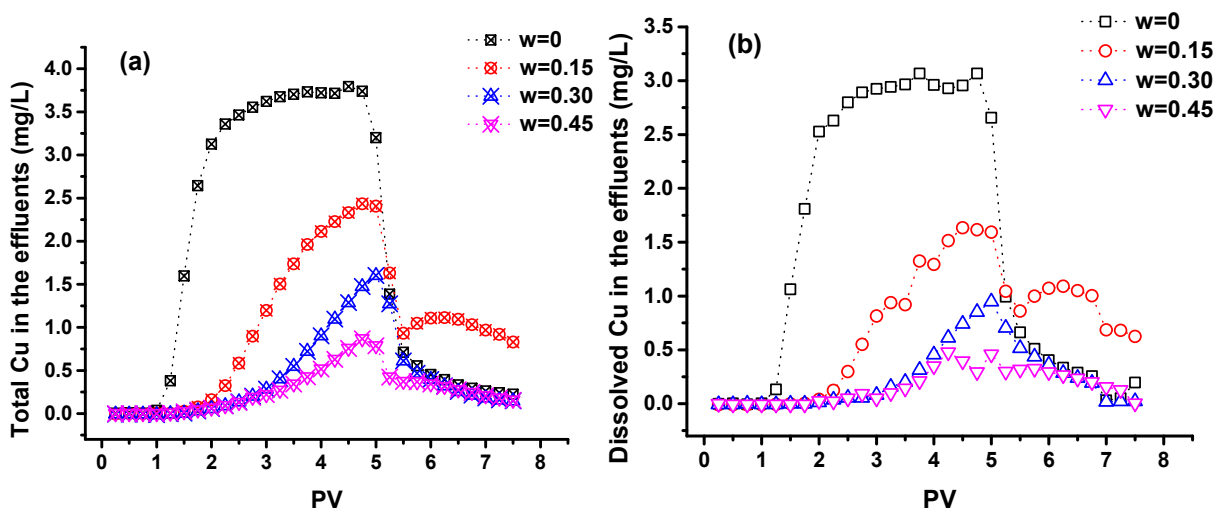


Figure S3. The total (a) and dissolved (b) concentrations of Cu in the effluents as a function of Fe oxide fraction (w) at pH 5.0 and 1 mM KCl.

Figure S4.

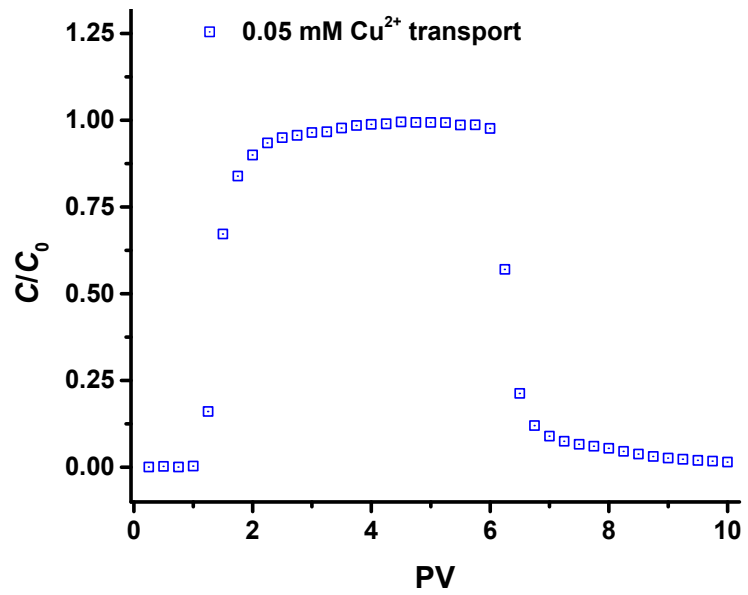


Figure S4. The breakthrough curve of 0.05 mM CuCl₂ in sand column ($\omega = 0$) at pH 5.0 and 1 mM KCl.

References

1. Wang, D.; Bradford, S.A.; Paradelo, M.; Peijnenburg, W.J.G.M.; Zhou, D. Facilitated transport of copper with hydroxyapatite nanoparticles in saturated sand. *Soil Science Society of America Journal* **2012**, *76*, 375-388, doi:10.2136/sssaj2011.0203.
2. Elimelech, M.; Nagai, M.; Ko, C.-H.; Ryan, J.N. Relative insignificance of mineral grain zeta potential to colloid transport in geochemically heterogeneous porous media. *Environmental Science & Technology* **2000**, *34*, 2143-2148, doi:10.1021/es9910309.
3. Schijven, J.F.; Šimůnek, J. Kinetic modeling of virus transport at the field scale. *Journal of Contaminant Hydrology* **2002**, *55*, 113-135, doi:https://doi.org/10.1016/S0169-7722(01)00188-7.
4. Bradford, S.A.; Simunek, J.; Bettahar, M.; van Genuchten, M.T.; Yates, S.R. Modeling colloid attachment, straining, and exclusion in saturated porous media. *Environmental Science & Technology* **2003**, *37*, 2242-2250, doi:10.1021/es025899u.
5. He, J.; Li, C.; Wang, D.; Zhou, D. Biofilms and extracellular polymeric substances mediate the transport of graphene oxide nanoparticles in saturated porous media. *Journal of Hazardous Materials* **2015**, *300*, 467-474, doi:https://doi.org/10.1016/j.jhazmat.2015.07.026.
6. He, J.; Wang, D.; Fang, H.; Fu, Q.; Zhou, D. Inhibited transport of graphene oxide nanoparticles in granular quartz sand coated with *Bacillus subtilis* and *Pseudomonas putida* biofilms. *Chemosphere* **2017**, *169*, 1-8, doi:https://doi.org/10.1016/j.chemosphere.2016.11.040.
7. Adamczyk, Z.; Siwek, B.; Zembala, M.; Belouschek, P. Kinetics of localized adsorption of colloid particles. *Advances in Colloid and Interface Science* **1994**, *48*, 151-280.